EFFECTS OF CYCLIC LOADING ON MECHANICAL PROPERTIES OF MAHA SARAKHAM SALT

Kittitep Fuenkajorn* **and Decho Phueakphum**

Received: Jan 22, 2009; Revised: Apr 22, 2009; Accepted: Apr 29, 2009

Abstract

Series of laboratory testing have been performed to assess the effects of cyclic loading on compressive strength, elasticity and time-dependency of the Maha Sarakham rock salt. Results from the cyclic loading tests indicate that the salt compressive strength decreases with increasing number of loading cycles, which can be best represented by a power equation. The salt elastic modulus decreases slightly during the first few cycles, and tends to remain constant until failure. It seems to be independent of the maximum loads within the range used here. Axial strain-time curves compiled from loci of the maximum load of each cycle apparently show a time-dependent behavior similar to that of creep tests under static loading. In the steady-state creep phase, the visco-plastic coefficients calculated from the cyclic loading test are about an order of magnitude lower than those under static loading. The salt visco-plasticity also decreases with increasing loading frequency. Surface subsidence and cavern closure simulated using parameters calibrated from cyclic loading test results are about 40% greater than those from the static loading results. This suggests that application of the property parameters obtained from the conventional static loading creep test to assess the long-term stability of storage caverns in salt with internal pressure fluctuation may not be conservative.

Keywords: Fatigue, creep, elasticity, strength, viscosity, salt

Introduction

Rock salt around storage caverns will be subject to cycles of loading due to the fluctuation of cavern pressures during product injection and retrieval periods. Depending on the types of stored products (e.g. petroleum, liquefied gas or compressed-air) and on the designed operating schemes, the injection-withdrawal durations can range from daily to annual, and the minimum and maximum cavern pressures can be as low as 20% and as high as 90% of the in-situ stresses at the casing shoe (cavern top). Due to the complexity of cavern ground geometry and the need to predict the future stability conditions (normally up to a few decades), the stability and operating pressures of the salt caverns have commonly been analyzed and designed via numerical modeling capable of handling time-dependent constitutive equations. A difficulty

Geomechanics Research Unit, Institute of Engineering, Suranaree University of Technology, Muang District, Nakhon Ratchasima 30000 Thailand. Tel.: 66-44-224-443; Fax.: 66-44-224-448; E-mail: kittitep@sut.ac.th

* *Corresponding author*

may arise in determining the representative properties of the salt under such cyclic loading states. Since the salt properties are loading path dependent (non-linear), the laboratory determined properties under static loads (as commonly practiced) may not truly represent the actual in-situ salt behavior under cyclic loading.

The effect of cyclic loading on the elasticity and strengths of geologic materials has long been recognized (Haimson, 1974; Allemandou and Dusseault, 1996; Bagde and Petros, 2005). A common goal of their studies is to determine the fatigue strength of the materials. It has been found that loading cycles can reduce the material strength and elasticity, depending on the loading amplitude and the maximum applied load in each cycle (Zhenyu and Haihong, 1990; Singh *et al*., 1994; Ray *et al*., 1999; Kodama *et al*., 2000). Rare investigation has, however, been made to identify the cyclic loading effect on the time-dependent properties and behavior of soft and creeping materials such as salt.

The objective of this research is to determine experimentally the effects of cyclic loading on compressive strength, elasticity, visco-elasticity and visco-plasticity of rock salt from the Maha Sarakham formation. The efforts primarily involve mechanical characterization testing, creep testing and compression testing under static and cyclic loads. Finite element analyses are performed to demonstrate the impact of cyclic loading on the deformation of salt around a compressed-air storage cavern.

Rock Salt Specimens

The specimens tested here were obtained from the Lower Salt members of the Maha Sarakham formation in the Sakhon Nakhon basin, northeastern Thailand. This salt unit is being considered as a host rock for compressed-air energy storage by the Thai Department of Energy. The rock salt is relatively pure halite with a slight amount (less than 1-2%) of anhydrite, clay minerals and ferrous oxide. The average crystal (grain) size is about 5 x 5 x 10 mm. Warren (1999) gives detailed descriptions of the salt and geology of the basin. The core specimens with a nominal diameter of 60 mm tested here were drilled from depths ranging between 250 and 400 m.

Sample preparation followed the ASTM D4543 standard practice, as much as practical. Twenty-four specimens (L/D = 2.5) were prepared for uniaxial compression tests, 76 specimens (L/D of 0.5) for Brazilian tension tests, 14 specimens (L/D = 2.5) for cyclic loading tests, and 10 specimens (L/D = 2.5) for uniaxial creep tests. The samples were cut and ground using saturated brine as lubricant. After preparation, the specimens were labeled and wrapped with plastic film. The specimen designation was identified. Prior to mechanical testing, visual examination was made to determine the type and amount of inclusions.

Characterization Testing

Uniaxial and triaxial compression and Brazilian tension tests were conducted to obtain data for the Maha Sarakham salt, and to determine the test parameters for the subsequent creep and cyclic loading tests. The test procedure followed relevant ASTM standard practices (ASTM D3967 and D7012). The elastic modulus (measured from unloading curves) of the salt is 25.2 ± 1.9 GPa and the Poisson's ratio is 0.37 ± 0.11. The uniaxial compressive and Brazilian tensile strengths are 34.7 ± 2.2 MPa and 1.5 ± 0.4 MPa. Figure 1 shows the stress-strain curves monitored during the tests. The triaxial compressive strength tests use confining pressures between 5.5 and 19.3 MPa. Based on the Coulomb criterion the internal friction angle is calculated as 39 degrees and the cohesion as 15 MPa (Figure 2). The Maha Sarakham salt strengths and elasticity obtained here agree reasonably well with those obtained elsewhere (e.g., Hansen *et al*., 1984).

Creep Testing

Short- and long-term uniaxial creep tests were performed to determine the time-dependent properties of the salt under isothermal condition. The test procedure followed the

ASTM D7070-08 standard practice. For the short-term testing, the applied constant axial stresses are relatively high, varying from 10 to 30 MPa with the maximum test duration of 7 hours. For the long-term testing, the applied stresses vary from 7.8 to 12.6 MPa with the maximum test duration up to 30 days. The short-term test results are used to calibrate the visco-elastic parameters, and the long-term results calibrate the visco-plastic coefficient of the salt. Figures 3 and 4 plot the axial strain as a function of time for the short- and long-term testing.

Cyclic Loading Testing

A series of uniaxial cyclic loading tests were performed on the 60 mm diameter salt core specimens using a servo-controlled universal testing machine (Figure 5). The maximum axial stresses vary among sp ecimens from 15.9 MPa to 34.6 MPa (about 40% to 100% of the

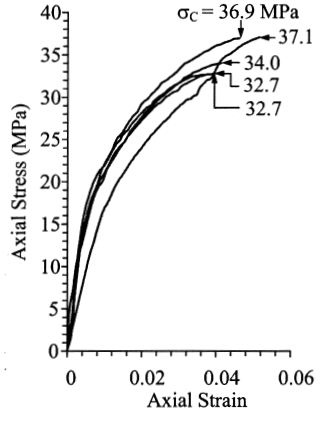

Figure 1. Results of uniaxial compressive strength testing. Numbers indicate stress at failure

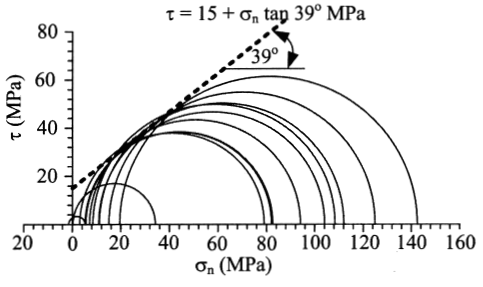

Figure 2. Mohr's circles and Coulomb criterion representing triaxial compressive strengths of Maha Sarakham Salt

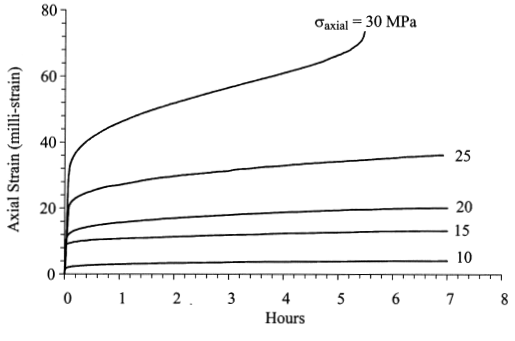

Figure 3. Results of the short-term uniaxial creep tests

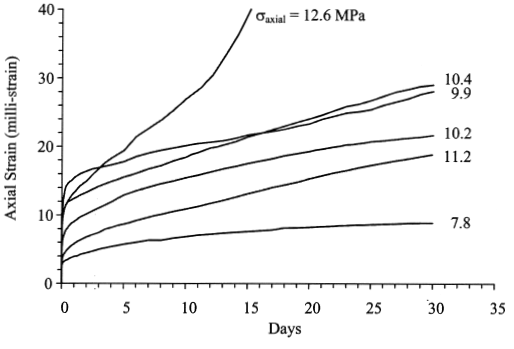

Figure 4. Results of the long-term uniaxial creep tests

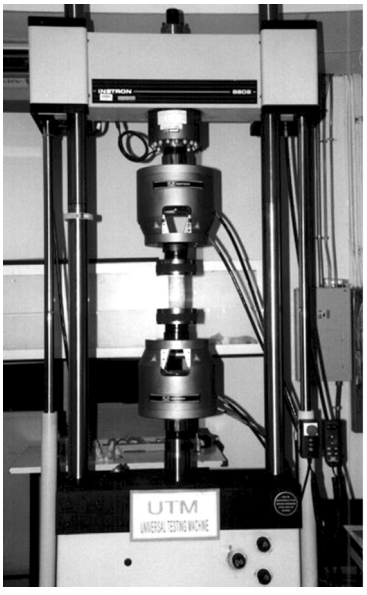

Figure 5. Salt specimen placed in the Universal Testing Machine (model FastTrack 8800, Instron Company) for uniaxial cyclic loading test

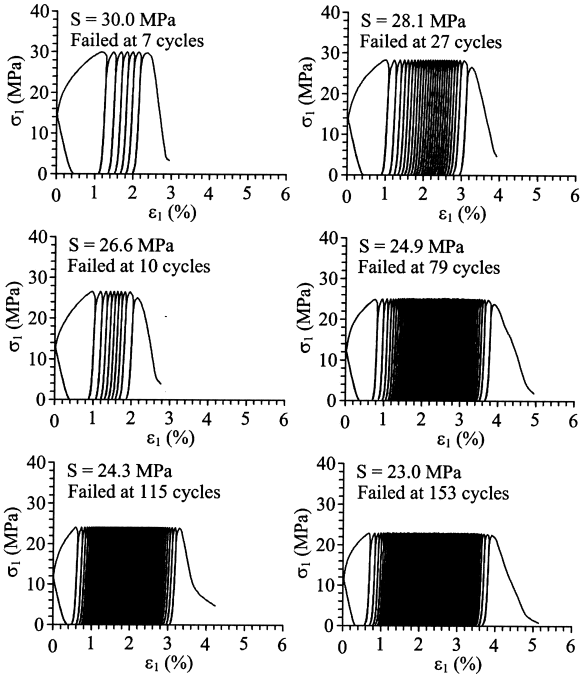

Figure 6. Examples of cyclic loading test results for loading frequency of 0.03 Hz. Axial stress (σ_1) plotted as a function of axial strain (ε_1). We can not explain why the machine records the decrease of axial strain in the first cycle

compressive strength) while the minimum stress was maintained constant at 0.15 MPa for all specimens. This small minimum stress is required to ensure that the ends of the specimen remain in contact with the loading platens during the test. The loading frequencies range from 0.001 Hz to 0.03 Hz. The accumulated axial strain, fatigue stress (S) and time were monitored during loading. Some examples of axial stress-strain curves measured during loading are given in Figure 6. Figure 7 shows the decrease of the failure (fatigue) stress as the number of loading cycle (N) increases, which can be represented by a power equation: $S = 32.33\ N^{(-0.07)}$. The behavior is similar to those obtained elsewhere for other geologic materials (Costin and Holcomb, 1981; Thoms and Gehle, 1982; Passaris, 1982; Bagde and Petros, 2004, 2005).

Figure 8 shows the axial strain-time curves compiled from loci of the loading cycles. The curves apparently show the transient, steady-state and tertiary creep phases which are similar to those obtained from the static creep testing. It is understood here that the transition point at which the strain rate changes from the steady-state phase (constant volume) to tertiary (volume increase) phase is corresponding to the dilation strength of the salt (DeVries *et al*., 2003). The loading cycles also exponentially decrease the dilation strength of the salt, as shown in Figure 7.

For each specimen, the elastic modulus values calculated from the series of unloading curves are plotted as a function of loading cycles in Figure 9. For all stress levels, the salt elasticity exponentially decreases as the number of loading cycles increases, and nearly remains constant after about 50 to 100 cycles. The calculated elastic modulus values range from 20 GPa to 35 GPa. They, however, tend to be independent of the applied maximum loads used

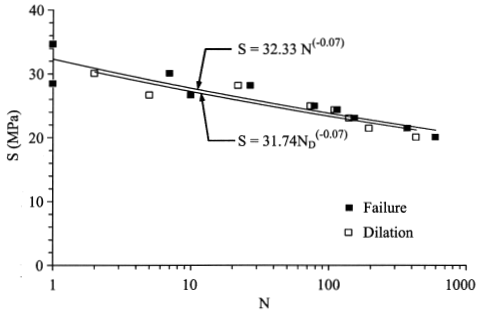

Figure 7. Fatigue strength (S) plotted as a function of numbers of loading cycles at failure (N) and at dilation (N_D)

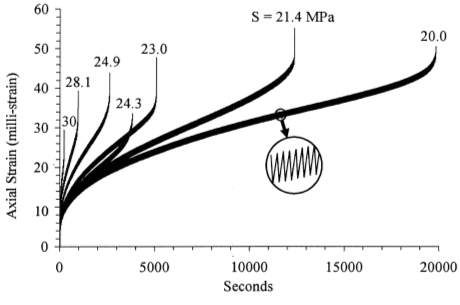

Figure 8. Axial strain-time curves from uniaxial cyclic loading tests

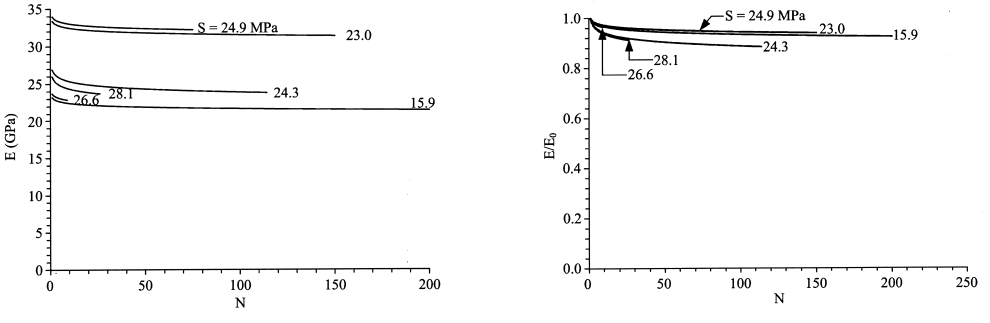

Figure 9. Elastic modulus, E (top) and normalized elastic modulus, E/E_0 (bottom) plotted as a function of number of loading cycles (N) up to failure

here, as also evidenced by the normalized elastics modulus (E/E_0) as a function of N in Figure 9, where E_0 is the modulus measured during the first loading cycle.

Salt Property Calibration

To assess the effect of cyclic loading on the time-dependent properties of salt, a simple rheological creep model is used to describe the constitutive behavior of the salt under isothermal condition. The modular components of the creep model are given in Figure 10. It is well recognized that several other constitutive models have been developed for describing the salt behavior (Jaeger and Cook, 1979). Some are very sophisticated and capable of handling complex thermo-mechanical behavior. The model used here, however, is simpler, and yet capable of disclosing the impacts of cyclic loading separately for the visco-elastic and the visco-plastic modes. It is probably more practical to analyze the problem under isothermal conditions. In Figure 10, G_1 and K_1 are shear and bulk modulus; G_2 and K_2 are shear and bulk modulus in visco-elastic mode; and η_2 and η_4 are visco-elastic and visco-plastic coefficients. These elastic and time-dependent parameters can be calibrated from the laboratory test results using a regression analysis (Fuenkajorn and Serata, 1992, 1994; Serata and Fuenkajorn, 1992).

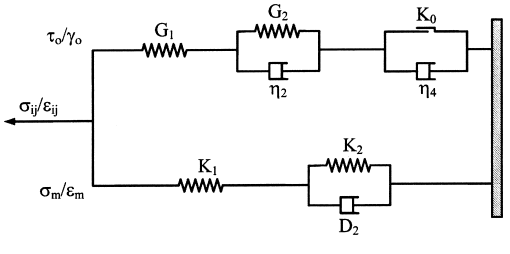

Figure 10. Modular representation of constitutive equations used here to describe the time-dependent behavior of salt (modified from Fuenkajorn and Serata, 1994)

The constitutive model separates the stress tensors into deviatoric (σ_{ij}) and volumetric ($\sigma_m\delta_{ij}$) parts. These are related to the strain tensors, ε_{ij} (deviatoric) and $\sigma_m\delta_{ij}$ (volumetric) through the rheological forms shown in Figure 10. The detailed constitutive relations are given by Serata *et al*. (1989) and Serata and Fuenkajorn (1992). The relations in elastic and visco-elastic states are as follows:

$$\sigma_{ij} = 2G_1\varepsilon_{ij} \tag{1}$$

$$\dot{\sigma}_{ij} + \frac{G_1 + G_2}{\eta_2}\sigma_{ij} = 2G_1\dot{\varepsilon}_{ij} + \frac{2G_1G_2}{\eta_2}\varepsilon_{ij} \tag{2}$$

where $\dot{\sigma}_{ij}$ and $\dot{\varepsilon}_{ij}$ are the time derivatives of the respective deviatoric stresses and strains (stress and strain rates).

When the octahedral shear stress (τ_o) exceeds the octahedral shear strength (K_o), the viscoplastic behaviour can be described by:

$$\ddot{\sigma}_{ij} + \left[\frac{G_1}{\eta_4} + \frac{G_1}{G_2} + \frac{G_2}{\eta_2}\right]\dot{\sigma}_{ij} + \frac{G_1G_2}{\eta_2\eta_4}\left[1 - \frac{K_o}{\tau_o}\right]\sigma_{ij} = 2G_1\ddot{\varepsilon}_{ij} + \frac{2G_1G_2}{\eta_2}\dot{\varepsilon}_{ij} \tag{3}$$

Here, $\ddot{\sigma}_{ij}$ and $\ddot{\varepsilon}_{ij}$ represent the second time derivatives of the tensors $\dot{\sigma}_{ij}$ and $\dot{\varepsilon}_{ij}$. The octahedral shear strength (K_o) is defined as:

$$K_o = \exp[-C(\gamma_o - \gamma_c/\gamma_c)] \tag{4}$$
$$[K^A + (K^B - K^A)\{1 - \exp(-\alpha\sigma_m)\}$$
$$-K^B\sigma_m/P] + K^B\sigma_m/P$$

where α is a yield surface coefficient and K^A and K^B are an unconfined octahedral shear strength and ultimate octahedral shear strength, C is the strain-softening coefficient varying from 0 to 1, γ_o is the induced octahedral shear strain, γ_c is the critical octahedral shear strain, and P is the plastic transition pressure. These parameters can be obtained from the regression of the laboratory test results. Table 1 summarizes the results obtained from the

regression analysis.

The visco-plastic coefficients calculated for both creep and cyclic loading tests is plotted as a function of the applied stress (calculated in terms of the octahedral shear stress, τ_{oct}) in Figure 11. The visco-plastic coefficients obtained from the creep testing are about 1-2 orders of magnitude higher than those from the cyclic loading. They decrease exponentially as the applied stresses increase, which can be best represented by: $\eta_4 = A \cdot \exp [B \cdot \tau_{oct}]$, where A and B are empirical constants.

A higher loading frequency results in a lower visco-plasticity of the salt. The constant A depends on the loading frequency (f) which can be determined from: $A = 25.2\, f^{(-0.18)}$. The exponent B tends to be constant at 0.7, independent of the loading frequency range used here (Table 2). By substituting the loading frequency equivalent to daily cycle ($f = 11.6 \times 10^{-6}$ Hz) into this equation, the constant A for the daily cycle operation can be calculated as 190 GPa.day, and the visco-plastic coefficient (η_4) becomes 1.8 GPa.day.

The axial strain-time curves obtained from the cyclic loading (as shown in Figure 8) also yield the critical octahedral shear strain (γ_c) for the salt. These strains correspond to the transition point from plastic creep (no volume change) in steady-state phase to dilation (volume increase) in the tertiary phase. The critical shear strain decreases exponentially with increasing octahedral shear stress. Figure 12 plots the measured γ_c as a function of τ_{oct}, and shows their empirical relation.

Table 1. Visco-elastic and visco-plastic coefficients obtained from creep and cyclic loading tests

Test methods	σ_1 (MPa)	τ_{oct} (MPa)	σ_{mean} (MPa)	η_2 (GPa.day)	η_4 (GPa.day)
Uniaxial creep test	7.8	3.7	2.6	1.200	29.100
	9.9	4.7	3.3	0.300	8.800
	10.2	4.8	3.4	1.000	8.700
	11.2	5.3	3.7	1.000	8.900
	11.4	5.4	3.8	0.700	7.400
	4.1	1.9	1.4	-	83.30
	7.1	3.3	2.4	-	53.40
	9.1	4.3	3.0	-	16.60
	11.1	5.2	3.7	-	12.10
	14.1	6.6	4.7	-	3.500
Cyclic loading test (f = 0.03 Hz)	20.0	9.4	6.7	0.011	0.064
	21.4	10.1	7.1	0.010	0.041
	23.0	10.8	7.7	0.006	0.022
	24.3	11.5	8.1	0.003	0.015
	24.9	11.7	8.3	0.003	0.012
	28.1	13.2	9.4	0.001	0.005
	30.0	14.1	10.0	-	0.002
Cyclic loading test (f = 0.001 Hz)	16.0	7.5	5.3	-	0.355
	21.6	10.2	7.2	-	0.075
	23.0	10.8	7.7	-	0.053
	27.0	12.7	9.0	-	0.010
	29.0	13.7	9.7	-	0.005

Numerical Simulation

A finite element analysis with the creep model above is performed to demonstrate the impact of cyclic loading on the salt behavior around a compressed-air storage cavern subjecting to daily cycles of pressure injection and retrieval. For this example, the cavern is an upright cylinder with a diameter of 50 m. The top and bottom of the cavern are at 500 m and 700 m depths. Figure 13 shows the finite element mesh for this example. The analysis is made in axial symmetry. The storage cavern model is subject to a maximum pressure of 80% (8.1 MPa) and a minimum pressure of 20% (2.0 MPa) of the in-situ stress at the cavern top. Two sets of property parameters are used, one calibrated from static loading tests, the other from cyclic loading tests. Table 3 summarizes the key parameters used in the simulations. The visco-plastic coefficient for the loading frequency equivalent to the daily cycle is used in the simulations. Since the long-term creep deformation of the storage cavern is the primary concern, the effect of loading frequency on the short-term properties (elastic and visco-elastic parameters) are not considered in the simulations. As a result, G_1, K_1, G_2, K_2, and η_2 are assumed to be independent of the loading frequency. The elastic and visco-elastic parameters as listed in Table 3 represent the average of the values calibrated from the test results. Both simulations assume a constant cavern pressure of 5.1 MPa which is averaged from the maximum and minimum storage pressures. The surface subsidence and cavern

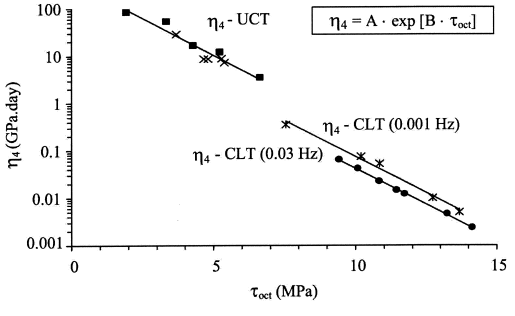

Figure 11. Visco-plasticity (η_4) as a function of octahedral shear stress (τ_{oct}) obtained from creep tests (UCT) and cyclic loading tests (CLT)

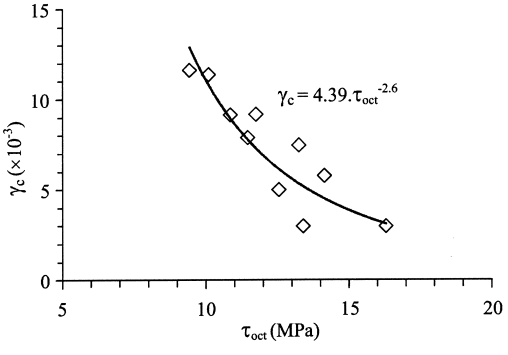

Figure 12. Octahedral shear strain (γ_c) as a function of octahedral shearstress (τ_{oct}) determined from cyclic loading tests

Table 2. Constants A and B for empirical equation: $\eta_4 = A \cdot \exp [B \cdot \tau_{oct}]$

Viscosity coefficients	Loading frequency, f (Hz)	A	B
Uniaxial Creep Test (UCT):			
- Visco-plasticity (η_4)	0.19×10^{-6}	382	-0.72
Uniaxial Cyclic Loading Test (CLT):			
- Visco-plasticity (η_4):	0.001	87	-0.71
- Visco-plasticity (η_4):	0.030	46	-0.70

closure induced by daily air injection-retrieval cycles during 12 months are calculated for the two cases.

Figure 14 shows the surface subsidence (above the center of the cavern) and cavern closure computed as a function of time during 12 months of the operation. The simulation using property parameters calibrated from the cyclic loading results shows subsidence and cavern closure of nearly twice that using the static loading results. The closure rate predicted from using cyclic loading parameters is higher than that from static loading parameters. This suggests that parameters derived from static loading may not be conservative for use in the simulation of salt storage caverns that are subject to repeated change of the internal pressure.

Discussions and Conclusions

The uniaxial cyclic loading tests as conducted here not only provide the fatigue stress and complete strain-time curves of the salt, but also reveal the dilation strength and critical shear strain of the rock. These parameters can not be easily obtained from the conventional test methods (i.e., the compressive strength test and creep test). The fatigue stress can help define the operational life of storage caverns in salt, which depends also on the loading cycles and the loading amplitudes (difference between the maximum and minimum storage pressures). The creep (viscosity) parameters are necessary to determine the time-dependent deformation of the surrounding salt. The critical strain and dilation strength define the maximum deformation before dilation strain or accelerated creep rate occurs under a given shear stress. This is useful for the design of the safe minimum internal pressure for a gas or compressed-air storage cavern in salt.

Under the test parameters used here, the cyclic loading can decrease the salt strength by up to 30%, depending on the maximum applied load and the number of loading cycles. The effect of loading frequency on the salt strength appears to be small as compared to the impacts

Table 3. Summary of property parameters used in numerical simulation

Key properties	Static loading	Cyclic loading
Elastic Parameters		
Elastic Modulus, E (MPa)	25.20	25.200
Poisson's Ratio, ν	0.37	0.370
Shear Modulus, G_1 (GPa)	10.20	10.200
Bulk Modulus, K_1 (GPa)	39.20	39.200
Visco-elastic Parameters		
Visco-elastic Shear Modulus, G_2 (GPa)	1.00	0.800
Visco-elastic Bulk Modulus, K_2 (GPa)	3.80	2.900
Visco-elastic Coefficient, η_2 (GPa.day)	0.50	0.007
Visco-plastic Parameter		
Visco-elastic Plastic Coefficient, η_4 (GPa.day)	3.40	1.800 (calculated for daily cycle)
Critical Octahedral Shear Strain, γ_c ($\times 10^{-3}$)	5.00	2.000

from the magnitudes of the maximum load and the loading amplitude. By using a simple isothermal creep model, the visco-elastic and visco-plastic coefficients of the salt can be determined from the static and the cyclic loading test results. Both parameters decrease exponentially with increasing applied octahedral shear stress. They also decrease with increasing loading frequency. The results from storage cavern simulations suggest that the property parameters obtained from the static (creep) tests can under-estimate the cavern deformation and surface subsidence as compared to those from the cyclic loading tests. This could lead to a non-conservative cavern design and stability analysis. The effect of loading frequency on the elastic modulus of the salt can not be detected here. This is probably because of the narrow range of the tested frequencies or the intrinsic variability among the salt specimens, or both.

Acknowledgment

This research is funded by Suranaree University of Technology. Permission to publish this paper is gratefully acknowledged.

References

Allemandou, X. and Dusseault, M.B. (1996). Procedures for cyclic creep testing of salt rock, results and discussions. Proceedings of the 3rd Conference on the Mechanical Behavior of Salt; Sept 14-16, 1993; Clausthal-Zellerfeld, Trans Tech Publications, p. 207-218.

ASTM D3967-86. Standard test method for splitting tensile strength of intact rock core specimens. In: Annual Book of ASTM Standards, American Standard Society for Testing and Materials, Philadelphia, PA. 04.08.

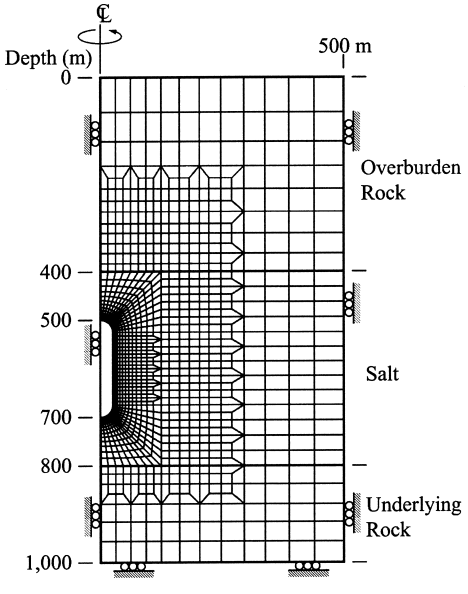

Figure 13. Finite element mesh constructed to simulate an example of storage cavern in salt

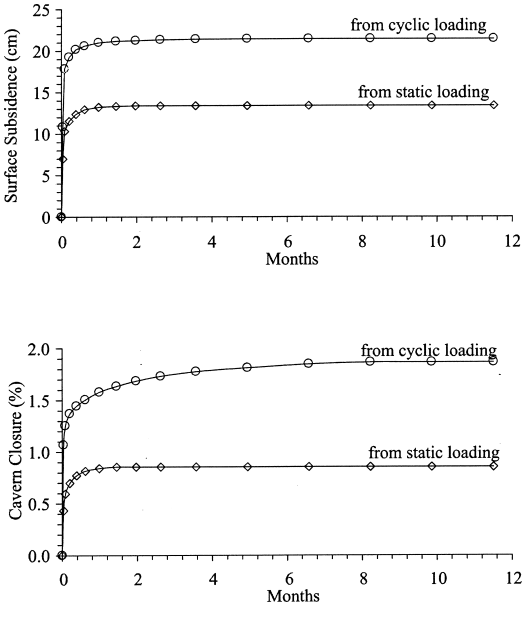

Figure 14. Surface subsidence (top) and cavern closure (bottom) using parameters from static and cyclic loading

ASTM D4543-08. Standard practice for preparing rock core specimens and determining dimensional and shape tolerances. In: Annual Book of ASTM Standards, American Standard Society for Testing and Materials, West Conshohocken, PA, 04.08.

ASTM D7012-07. Compressive strength and elastic moduli of intact rock core specimens under varying states of stress and temperatures. In: Annual Book of ASTM Standards, American Standard Society for Testing and Materials, West Conshohocken, PA, 04.08.

ASTM D7070-08. Creep of rock core under constant stress and temperature. In: Annual Book of ASTM Standards, American Standard Society for Testing and Materials, West Conshohocken, PA, 04.08.

Bagde M.N. and Petros, V. (2004). Experimental investigation into fatigue behaviour of intact sandstone and conglomerate rock types in uniaxial dynamic cyclic loading. Geophysical Research Abstracts, 6: 07240.

Bagde, M.N. and Petros, V. (2005). Fatigue properties of intact sandstone samples subjected to dynamic uniaxial cyclical loading. International Journal of Rock Mechanics and Mining Sciences, 42(2): 237-250.

Costin, L.S. and Holcomb, D.J. (1981). Time-dependent failure of rock under cyclic loading. Tectonophysics, 79(3-4):279-296.

DeVries, K.L., Mellegard, K.D., and Callahan, G.D. (2003). Laboratory testing in support of a bedded salt failure criterion. SMRI: Fall 2003 meting, 5-8 October 2003, Chester, United Kingdom, England.

Fuenkajorn, K. and Serata, S. (1992). Geohydrological Integrity of CAES in Rock Salt," Compressed-Air Energy Storage: Proceedings of the Second International Conference, Electric Power Research Institute, San Francisco, CA, July 7-9, 1992, p. 4.1-4.21.

Fuenkajorn, K. and Serata, S. (1994). Dilation-induced permeability increase around caverns in rock salt. Proceedings of the 1st North American Rock Mechanics Symposium; Jun 1-3, 1994; University of Texas at Austin, A.A Balkema, Rotterdam, p. 648-656.

Haimson, B.C. (1974). Mechanical behavior of rock under cyclic loading. Proceedings of the 3rd Congress of the International Society for Rock Mechanics, Part A. Advances in Rock Mechanics: Report of Current Research; Sept 1-7, 1974; Denver, National Academy of Sciences, Washington, D.C., p. 373-387.

Hansen, F.D., Mellegard, K.D., and Senseny, P.E. (1984). Elasticity and strength of ten natural rock salts. Proceeding of the 1st Conference on the Mechanical Behavior of Salt; Nov 9-11, 1981; The Pennsylvania State University, Trans Tech Publications: Clausthal Germany, p. 71-83.

Jaeger, J.C. and Cook, N.G.W. (1979). Fundamentals of Rock Mechanics. 3rd ed. Chapman and Hall, London, 475p.

Kodama, J., Ishizuka, Y., Abe, T., Ishijima, Y., and Goto, T. (2000). Estimate of the fatigue strength of granite subjected to long-period cyclic loading. Shigen-to-Sozai, 116:111-118.

Passaris, E.K.S. (1982). Fatigue characteristics of rock salt with reference to underground storage caverns. Proceedings ISRM Symposium on Rock Mechanics: Caverns and Pressure Shafts; May 26-28, 1982; Aachen, Germany, Taylor & Francis Group, p. 983-989.

Ray, S.K., Sarkar, M., and Singh, T.N. (1999). Effect of cyclic loading and strain rate on the mechanical behaviour of sandstone. Int. J. Rock Mech. Min. Sci., 6(4):543-549.

Serata, S. and Fuenkajorn, K. (1992). Formulation of a constitutive equation for salt. Proceedings of the Seventh International Symposium on Salt; April 6-9, 1992; Kyoto, Japan, Elsevier Science Publishers,

p. 483-488.

Serata S., Mehta, B., and Hiremath, M. (1989). Geomechanical stability analysis for CAES cavern operation. Proceedings of the International Conference on Storage of Gases in Rock Caverns; June 26-28, 1989; Trondheim, Norway, Rotterdam, p.129-136.

Singh, T.N., Ray, S.K., and Singh, D.P. (1994). Effect of uniaxial cyclic compression on the mechanical behaviour of rocks. Indian J. Eng. Mater. Sci., 1(2):118-120.

Thoms, R.L. and Gehle, R. (1982). Experimental study of rock salt for compressed air energy storage. Proceedings ISRM Symposium on Rock Mechanics: Caverns and Pressure Shafts; May 26-28, 1982; Aachen, Germany, Taylor & Francis Group, p. 991-1002.

Warren, J. (1999). Evaporites: Their Evolution and Economics. Blackwell Science, Oxford, 438p.

Zhenyu, T. and Haihong, M. (1990). An experimental study and analysis of the behaviour of rock under cyclic loading. Int. J. Rock Mech. Min. Sci., 27(1):51-56.